Exciplex dynamics in a blend of π-conjugated polymers with electron donating and accepting properties: MDMO-PPV and PCNEPV

Ton Offermans, Paul A. van Hal, and Stefan C. J. Meskers*
Molecular Materials and Nanosystems, Department of Chemical Engineering and Chemistry, Eindhoven University of Technology, P.O. Box 513, 5600 MB Eindhoven, The Netherlands and Dutch Polymer Institute (DPI), P.O. Box 902, 5600 AX Eindhoven, The Netherlands

Marc M. Koetse
TNO Science and Industry, P.O. Box 6235, 5600 HE Eindhoven, The Netherlands and Dutch Polymer Institute (DPI), P.O. Box 902, 5600 AX Eindhoven, The Netherlands

René A. J. Janssen
Molecular Materials and Nanosystems, Departments of Applied Physics and Chemical Engineering and Chemistry, Eindhoven University of Technology, P.O. Box 513, 5600 MB Eindhoven, The Netherlands
(Received 9 February 2005; revised manuscript received 17 May 2005; published 19 July 2005)

The photophysical properties of a solution processed blend of two semiconducting polymers with electron donating and electron accepting properties, respectively, as used in polymer photovoltaic devices have been investigated. We show that in the binary mixture of poly[2-methoxy-5-(3,7-dimethyloctyloxy)-1,4-phenylenevinylene] (MDMO-PPV) and poly[oxa-1,4-phenylene-(1-cyano-1,2-vinylene)-(2-methoxy-5-(3,7-dimethyloctyloxy)-1,4-phenylene)-1,2-(2-cyanovinylene)-1,4-phenylene] (PCNEPV) photoexcitation of either one of the polymers results in formation of a luminescent exciplex at the interface of the two materials. Photoinduced absorption spectroscopy shows that this exciplex can decay to the lowest triplet state (T_1) of MDMO-PPV. Application of an electric field results in dissociation of the marginally stable exciplex into charge carriers, which provides the basis for the photovoltaic effect of this combination of materials. Spin allowed recombination of the charge carriers to the MDMO-PPV T_1 state is invoked to explain the field-enhanced quantum yield for triplet formation observed by photoinduced reflection measurements on photovoltaic devices made from the composite films. The field enhanced triplet yield is identified as loss mechanism for the photovoltaic performance of this combination of materials.

DOI: 10.1103/PhysRevB.72.045213 PACS number(s): 78.55.Kz, 73.50.Pz, 73.20.−r, 78.66.Qn

I. INTRODUCTION

Photoinduced charge transfer in blends of π-conjugated polymers with complementary *p*- and *n*-type semiconducting properties is being studied intensively, motivated by the possibility to utilize these composite layers in photovoltaic devices. In fact, the use of two materials with complementary *p*- and *n*-type electronic properties is crucial to the operation of any polymer solar cell because photoexcitation of a pure conjugated polymer generally provides a bound electron-hole pair or exciton rather than free charges.[1] However, the charge carriers required for the photovoltaic effect can be created in high yield in a photoinduced charge transfer at the interface of donor (*p*-type) and acceptor (*n*-type) materials with appropriately positioned energy levels.[2,3] Surprisingly high efficiencies (>50%) for collection of photoinduced charge carriers with respect to incident photons have been observed in bulk heterojunction photovoltaic devices that use an active layer of a π-conjugated polymer blended with a fullerene derivative.[4–7] In these blends, neutral excitons resulting from photon absorption by one of the two components diffuse to the interface, where dissociation into charge carriers can occur. It is well established that the microscopic structure of the bulk heterojunction is crucial to the performance of the device because intimate mixing ensures efficient charge generation and because the two phases should provide percolating pathways for both photogenerated charge carriers to opposite electrodes. The morphologies of the various composite layers have been analyzed in detail and blends that show phase segregation of the electron donating and accepting material with a typical length scale of in the range of 10–100 nm show optimal photovoltaic performance.[8–12]

Following charge generation at an interface, the charges have to be separated spatially and escape from recombination before they can be transported and collected at the electrodes. However, given the relatively low dielectric constant of organic molecules and polymers, one expects that the charge carriers will be relatively strongly bound by the Coulomb force. In fact, the process leading to generation of free charges inside these organic materials is presently only partly understood.[13–18] It has been shown that a built-in electrical field, resulting from the use of two electrodes with different work functions, is essential to collect the charges generated at the interface efficiently.[19]

At present it is not entirely known which criteria the electron accepting and donating materials have to fulfill to ensure efficient separation of the initial geminate charge pairs into free charge carriers. Moreover, in polymer blends a special type of excitation may exist that occurs uniquely at the interface between electron donating and accepting material.

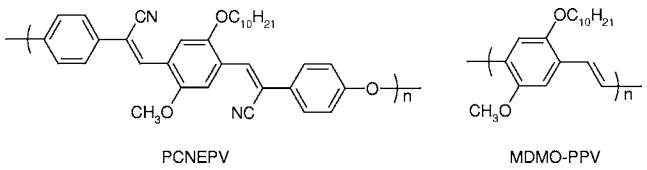

FIG. 1. Structure of PCNEPV and MDMO-PPV.

The excitation has a charge-transfer character and may in a very crude approximation be viewed as a hole on the electron donating material and an electron on the electron accepting material bound together by the Coulomb attraction between these two quasiparticles. Such states are often referred to as exciplexes.

The formation of excited-state complexes or exciplexes has been investigated in detail for aromatic molecules in solution.[20,21] After photoexcitation of certain aromatic molecules and collision of these excited molecules with a second molecule with strong electron donating or accepting properties, a complex can be formed which is stable only in the excited state and that can often be observed by a characteristic emission at a photon energy that is lower than the emission of either of the two components. This exciplex derives its stability from delocalization of the electronic excitation over the two molecules and from partial electron transfer between the donating and accepting molecule. The charge-transfer character of this exciplex has been found to increase with the strength of the electron donating properties of the one component and with the electron affinity of the other. The occurrence of exciplex-type emission in bends of π-conjugated polymers is a relatively recent discovery. In heterojunctions of polymer-polymer blends redshifted emission has been observed and attributed to an exciplex state.[22–24] Efficient red-emitting LEDs can be made based on exciplex emission from mixtures of donor and acceptor polymers.[22,23]

Here we investigate the photophysical processes associated with the exciplex in a MDMO-PPV:PCNEPV bulk heterojunction device. The chemical structure of MDMO-PPV and PCNEPV (Refs. 25 and 26) are shown in Fig. 1. PCNEPV has a relatively high electron affinity due to the strongly electron withdrawing cyano substituents and functions as the electron accepting component in the blend. PCNEPV is a derivative of CN-PPV, for which charge transfer has been shown in MEH-PPV:CN-PPV blends.[2] PCNEPV has also been used in bilayer photovoltaic devices blended with MEH-PPV on TiO_2.[27] Photovoltaic devices based on the MDMO-PPV:PCNEPV blends reach power conversion efficiencies up to 0.75% under standard conditions (AM1.5, 1000 W/m^2) after thermal annealing and a maximum efficiency for the conversion of incident photons into collected electrons (IPCE) of 23% at photon energies of 2.48 eV.[28] For the blends under study, phase segregation with typical length scales of 20–50 nm could be observed by TEM after thermal annealing of the film. For the untreated film, no phase segregation could be observed by atomic force microscopy (AFM).[28] The IPCE for the films that have not been annealed is lower than for the treated films (8–10 % at 2.48 eV). The photovoltaic effect in the untreated films indicates that also in these films phase segregation occurs to some extent. The cells are further characterized by a relatively high open circuit voltage of 1.3–1.4 V,[28] that stems from the relatively large separation between the valence-band level of MDMO-PPV and the conduction-band level of PCNEPV. The IPCE value of 23% leaves no doubt that absorption of light results in generation of charge carriers in this blend but we show that photoexcitation of a MDMO-PPV:PCNEPV blend also results in the formation of a luminescent exciplex. Herein we demonstrate that a relatively low electric field suffices to dissociate a significant fraction of this exciplex into free charge carriers, allowing for photovoltaic energy conversion. The exciplex can also decay to a lower-lying triplet excited state associated with MDMO-PPV. Such field-enhanced triplet formation may ultimately be one of the factors limiting solar cell performance of polymer-polymer bulk heterojunctions.

II. EXPERIMENT

Poly[oxa-1,4-phenylene-(1-cyano-1, 2-vinylene)-(2-methoxy-5-(3,7-dimethyloctyloxy)-1,4-phenylene)-1, 2-(2-cyanovinylene)-1,4-phenylene] (PCNEPV) was synthesized according to literature procedures.[25,26] The material used for this study had a weight average molecular weight (M_w) of 48 kg/mol with a polydispersity index (PDI) of 4 as measured by size-exclusion chromatography (SEC) versus polystyrene standards. Poly[2-methoxy-5-(3,7-dimethyloctyloxy)-1,4-phenylenevinylene] (MDMO-PPV, M_w=570 kg/mol and PDI=5) was synthesized via the sulfonyl route.[29] Composite MDMO-PPV:PCNEPV films were spin coated from chlorobenzene containing 0.25 wt % of each component. Prior to spin coating the solution was stirred at 70 °C for 1 h. The resulting films had a thickness of 40 nm as determined by profilometry (Tencor P10). Some measurements were carried out on annealed films. These films were annealed at 120 °C in a N_2 atmosphere for 15 min. Devices were prepared using glass substrates with patterned indium tin oxide (ITO) (Philips Research). After careful scrubbing, cleaning, and UV-ozone treatment, a 60-nm-thin layer of poly(3,4-ethylenedioxythiophene:poly(styrene sulfonate) (PEDOT:PSS) (Baytron P, H.C. Starck) was applied by spin coating, followed by the MDMO-PVV:PCNEPV blend. The metal back electrode of LiF (1 nm) and Al (150 nm) was evaporated at 10^{-7} mbar through a shadow mask. By this way four devices were created per substrate with areas of 0.095, 0.167, 0.37, and 1.03 cm^2, respectively. The 0.095-cm^2 and 0.37-cm^2 devices were used for photoinduced absorption measurements, the 0.167-cm^2 devices were used for time-resolved fluorescence measurements.

UV/vis absorption and fluorescence spectra were recorded with a Perkin-Elmer Lambda 900 spectrometer and an Edinburgh Instruments FS920 double-monochromator luminescence spectrometer using a Peltier-cooled red-sensitive photomultiplier, respectively. Films deposited on quartz substrates were used for UV/vis and fluorescence measurements. Time-correlated single-photon counting fluorescence studies were performed using an Edinburgh Instruments

LifeSpec-PS spectrometer. This instrument comprises a 400-nm (3.10-eV) picosecond laser (PicoQuant PDL 800B) operated at 2.5 MHz and a Peltier-cooled Hamamatsu microchannel plate photomultiplier (R3809U-50).

Near steady state photoinduced absorption (PIA) spectra were recorded between 0.35 and 3.00 eV by exciting with 2.70-eV photons from a mechanically modulated (275-Hz) cw Ar^+ laser. The resulting change in transmission (ΔT) of a tungsten halogen probe light through the sample was monitored with a phase-sensitive lock-in amplifier after dispersion by a grating monochromator and detection using Si, InGaAs, and cooled InSb detectors. The pump power incident on the sample was typically 25 mW with a beam diameter of 2 mm. The PIA ($-\Delta T/T$) was directly calculated from the change in transmission after correction for the photoluminescence. Photoinduced absorption spectra and photoluminescence spectra were recorded with the pump beam in a direction almost parallel to the direction of the probe beam. For measurement on devices, the probe beam was detected after reflection at the back electrode of the device at an angle of 45° to the incident probe beam. Temperature was controlled between 80 and 300 K with an Oxford Optistat cryostat.

J-V characteristics of the devices were measured with a Keithley 2400 source measuring unit in a N_2 atmosphere using "white" light illumination by a tungsten halogen lamp in combination with a KG1 infrared and a GG385 UV filter. The resulting illumination density was 75 mW/cm^2. The photocurrent was also measured using a modulated excitation (77 Hz) with 2.70-eV photons with intensity 0.8 W/cm^2 from the Ar^+ laser used in the PIA measurements, under background light illumination from a tungsten halogen lamp with similar intensity. The current was evaluated by measuring the amplitude of the oscillating voltage over a probe resistance R_S(0.01 Ω) connected in series with the device using a lock-in amplifier. The driving voltage over the device was applied using a Keithley 2400 source measuring unit. During the measurement the device was held in a vacuum using an Oxford Optistat cryostat, at room temperature or at 80 K.

The femtosecond laser system used for pump-probe experiments consisted of an amplified Ti/sapphire laser (Spectra Physics Hurricane), providing 150-fs pulses at 800 nm with an energy of 750 μJ and a repetition rate of 1 kHz. The pump pulses at 510 nm (2.43 eV) were created via optical parametric amplification (OPA) of the 800 nm and frequency doubling. The probe beams at 2200 nm (0.56 eV) and 980 nm (1.27 eV) were generated in a separate OPA. The pump beam was linearly polarized at the magic angle (54.7°) with respect to the probe beam, to cancel out orientation effects in the measured dynamics. The temporal evolution of the differential transmission was recorded using a cooled InSb detector (at 0.56 eV) or a Si detector (at 1.27 eV) by a standard lock-in technique at 500 Hz.

III. RESULTS

A. Exciplex formation in MDMO-PPV:PCNEPV films and photovoltaic devices

Figure 2 shows the optical absorption and fluorescence spectra for thin films of PCNEPV, MDMO-PPV, and their 1:1 wt blend. PCNEPV shows an absorption in the blue part of the spectrum with a maximum at 2.72 eV and an absorption coefficient $\alpha = 1.5 \times 10^5$ cm^{-1}. The onset of absorption of PCNEPV at 2.4 eV is at considerably lower energy than for the corresponding polymer without cyano substituents (PPV ether) at 2.8 eV.[30] In contrast, CN-PPV, which lacks the ether linkages, shows an onset at already 2.1 eV.[31] PCNEPV films show a bright yellow fluorescence with a maximum at 2.12 eV. The fluorescence maximum shows a large shift from the absorption maximum, which was also found for CN-PPV and may be related to the charge transfer (CT) character of the excitation arising from the presence of the strongly electron withdrawing cyano moieties. The lifetime of the fluorescence is exceptionally long for a conjugated polymer: $\tau = 14$ ns (Fig. 3). For the related CN-PPV a lifetime of 5.6 ns has been reported[32] and these long lifetimes have been rationalized to result from an interchain excitation.[32] MDMO-PPV shows an absorption maximum at 2.4 eV with $\alpha = 1.1 \times 10^5$ cm^{-1}. The onset of absorption occurs at 2.1 eV which shows that of the two polymers in the blend, MDMO-PPV has the lowest excited singlet state (S_1). For the pure

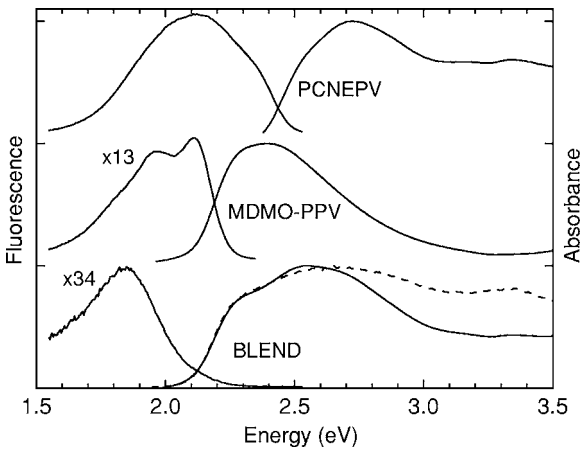

FIG. 2. Normalized UV-vis absorption and emission spectra of films of PCNEPV, MDMO-PPV, and the 1:1 wt % blend at room temperature (excitation at 2.29 eV). The excitation spectrum of the emission at 1.85 eV for the blend is shown by the dashed line.

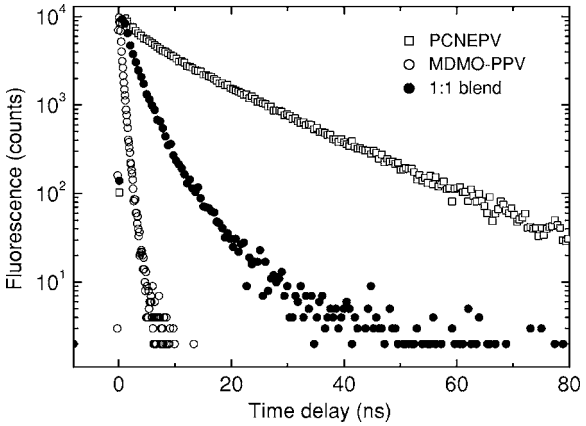

FIG. 3. Time-resolved emission of PCNEPV, MDMO-PPV, and the 1:1 wt % blend. Photoexcitation at 3.10 eV, detection at 1.90 eV.

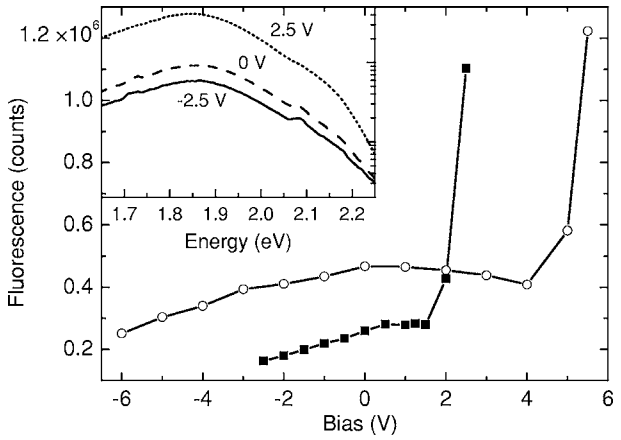

FIG. 4. Light emission of an ITO/PEDOT:PSS/MDMO-PPV:PCNEPV/LiF/Al device at a photon energy of 1.90 eV at different bias voltages, recorded with photoexcitation at 3 eV at room temperature (solid squares) and 80 K (open circles). The inset shows the emission spectra for three different voltages at room temperature.

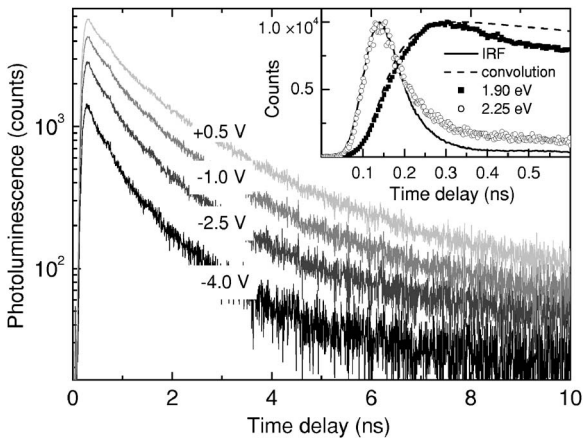

FIG. 5. Time-resolved emission of an ITO/PEDOT:PSS/MDMO-PPV:PCNEPV/LiF/Al device at different applied voltages recorded after photoexcitation 60 ps (full width at half maximum) pulses at 3.10 eV and detected at 1.90 eV. For clarity, the traces are offset vertically. The inset compares the instrument response function (IRF) (solid line) with the grow-in of the emission at 1.90 eV at V_{oc} (squares), the convolution of the IRF with $[\exp(-t/1.4)]$, $t>0]$ (dashed line) and the grow-in of the decay at 2.25 eV at V_{oc} (circles). The measurements were performed at room temperature.

MDMO-PPV film we observe the first vibronic in the fluorescence at 2.11 eV. The fluorescence lifetime of MDMO-PPV is $\tau=0.36$ ns (Fig. 3).

The absorption spectrum for the 1:1 wt blend (Fig. 2) shows that both polymers contribute to the absorption spectrum that peaks at 2.55 eV. In comparison with films of PCNEPV, the maximum intensity of the photoluminescence from the blend is reduced by a factor 34 and by a factor of 3 compared to MDMO-PPV. Interestingly, the spectral position of the emission differs from the fluorescence spectra of MDMO-PPV and PCNEPV. This different type of emission has its maximum intensity at 1.85 eV. The excitation spectrum of the blend (dotted line in Fig. 2) shows that the new emission can be generated via excitation of both MDMO-PPV and PCNEPV. By taking the ratio between the amplitudes in the excitation spectrum and the absorption spectrum, the dependence of the quantum yield of luminescence on excitation photon energy can be evaluated. From the data, it follows that the anomalous red emission in the mixture is generated more efficiently at excitation photon energies $E>2.8$ eV when compared to $E<2.8$ eV. After pulsed excitation, the emission initially decays with a lifetime $\tau=1.6$ ns. Apparently, the luminescent excited state in the blend has a *longer* lifetime than the S_1 state of MDMO-PPV but a *shorter* lifetime than the S_1 state of PCNEPV (see Fig. 3). We assign the photoluminescence at 1.85 eV to originate from an exciplexlike excited state formed at the interface between the electron donating and accepting polymers. Such exciplexes have previously been reported for a number of polymer-polymer combinations.[22–24]

The exciplex emission of the MDMO-PPV:PCNEPV blend can also be observed when the polymer layer is embedded in a device structure with a PEDOT:PSS bottom contact and a LiF/Al top contact (see Sec. II). We find that the intensity of the photoluminescence (PL) in these structures depends on the bias voltage applied over the device (Fig. 4). At room temperature, the intensity of the luminescence decreases when applying a voltage lower than the built-in potential (V_{bi}). At the low light intensities used in the PL measurements, the internal electric field inside the device vanishes when the difference in work function of the two electrodes used ($V_{bi}=0.9$ V) is compensated by an externally applied voltage.[33] This decrease of the PL indicates that the exciplex splits up into a pair of oppositely charged carriers under the influence of the electric field inside the device. Under forward bias, however, the intensity increases sharply for voltages >2 V. This rapid increase arises from electroluminescence. The spectra of the electroluminescence and the photoluminescence at low voltages are almost identical (see the inset in Fig. 4). At low temperature (80 K), the exciplex luminescence increases. Again the intensity is dependent on the applied bias and a maximum in intensity occurs close to the built-in voltage, meaning that the field-enhanced exciplex dissociation occurs under forward *and* reverse bias as expected. At low temperature the electroluminescence sets in at higher values of the applied bias (5 V), because injection of charges is more difficult at lower temperatures.

In Fig. 5 we show the results of a time-resolved luminescence experiment on the polymer blend in a device structure ($T=298$ K). The graph shows that the lifetime of the exciplex emission also depends on the applied bias. At more negative bias we observe a reduction of the lifetime of the exciplex emission. The inset in Fig. 5 shows the early time domain of the experiment. At 2.25 eV, where the MDMO-PPV emits, we observe a very weak emission (see also Fig. 2) that rises and decays in the same manner as the response function of the instrument. This indicates that the lifetime of the residual MDMO-PPV emission is much shorter than the instrument response (<100 ps). Hence we conclude that singlet photoexcitations in MDMO-PPV (which have a natural lifetime of 0.36 ns) diffuse towards the interface with the PCNEPV, where they are converted into exciplexes. This

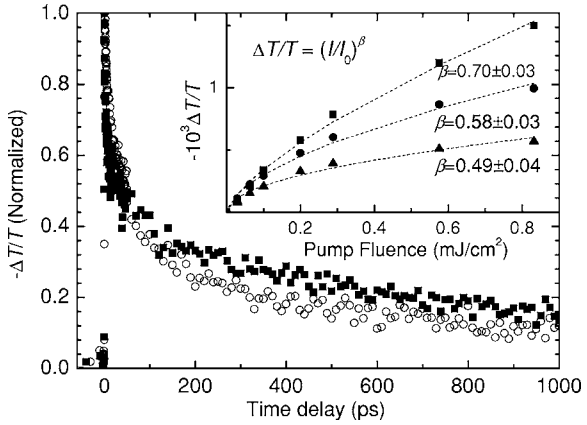

FIG. 6. Transient absorption spectra of the 1:1 wt % MDMO-PPV:PCNEPV blend pumped at 2.43 eV and probed at 1.27 eV (high-energy cation band, solid squares) and at 0.56 eV (low-energy cation band, open circles). The inset shows the pump intensity dependence of the transient absorption signals at 1.27 eV nm at 1 ps (squares), 50 ps (circles), and 500 ps (triangles) after excitation.

process occurs at times shorter than 100 ps after photoexcitation. The more intense exciplex emission (measured at 1.90 eV) rises more slowly than the residual MDMO-PPV emission. The rise can be modeled with a convolution of the instrument response and an exponential decay function with a 1.4-ns decay time (dashed line in the inset of Fig. 5). This demonstrates that the majority of exciplexes are formed within a time period much shorter than 100 ps after excitation. The fluorescence measurements are consistent with formation of the exciplex out of MDMO-PPV (and PCNEPV) excitations that have diffused towards the interface.

In additional experiments on shorter time scales, using subpicosecond pump-probe spectroscopy, we were able to probe photoinduced absorption transients at 0.56 and 1.27 eV after photoexcitation (200 fs) with 2.43-eV photons. These probe energies correspond to the low- and high-energy absorptions of MDMO-PPV radical cations, as will be shown later. The absorption traces pertaining to 0.56 and 1.27 eV (Fig. 6) exhibit the same temporal evolution and rise within the time resolution of the experimental setup ($\sim$0.3 ps). Bimolecular exciton-exciton annihilation at short delays is evident from the pump intensity dependence of $\Delta T/T$ (inset of Fig 6). However, following this rapid decay the induced absorption shows a slow decay with a time constant $\sim$1 ns. We assign the relatively slowly decaying photoinduced absorption signals to exciplexes. Incidentally, the almost identical decay of the induced absorption traces at 0.56 and 1.27 eV indicates that MDMO-PPV triplet states [which do absorb at 1.27 eV (see below), but not at 0.57 eV] are not formed to a significant extent in the 0–1-ns time domain.

B. Long-lived photoexcitations in MDMO-PPV:PCNEPV films and photovoltaic devices

Long-lived excitations such as triplet states and radical ions with lifetimes in the microsecond to millisecond range can be investigated by monitoring the photoinduced absorption (PIA) with mechanically modulated excitation and

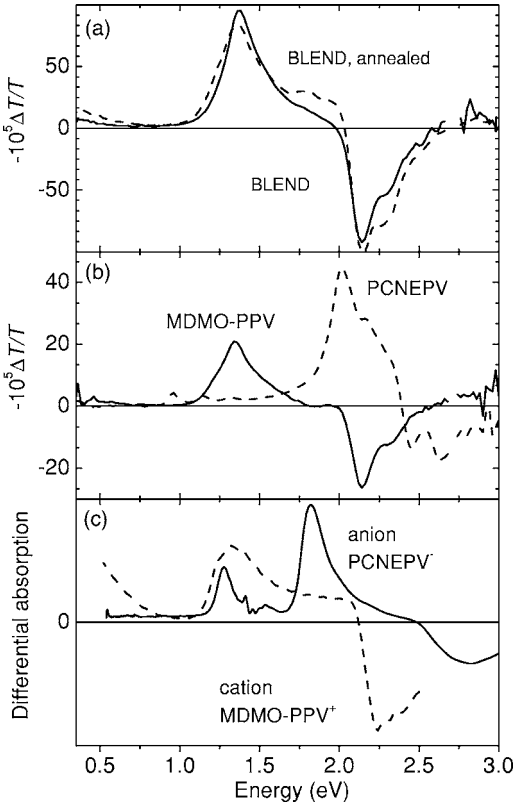

FIG. 7. (a) PIA spectra of a MDMO-PPV:PCNEPV blend (1:1 wt) before (solid line) and after thermal annealing (dashed line). (b) PIA spectra of MDMO-PPV (solid line) and PCNEPV (dashed line). (c) Spectroelectrochemistry of PCNEPV dissolved in THF at −1310 mV vs Fc/Fc^+ (solid line) at room temperature and PIA spectrum of a MDMO-PPV/PCBM blend (dashed line). All PIA spectra were recorded at 80 K with excitation at 2.70 eV, using a modulation frequency of 275 Hz.

lock-in detection (see Sec. II for details). For the materials under study the results of these experiments are shown in Fig. 7. The PIA spectrum of pristine MDMO-PPV [Fig. 7(b)] exhibits a triplet absorption band ($T_n \leftarrow T_1$) band centered at 1.35 eV and a bleaching band at 2.14 eV.[34] The PIA spectrum of pristine PCNEPV [Fig. 7(b)] shows a bleaching band above 2.4 eV, a large triplet absorption band at 2.02 eV,[35] and three smaller bands at 0.95, 1.15, and 1.34 eV that are also attributed to the triplet absorption because they show the same modulation frequency and pump power dependence as the absorption at 2.02 eV. We also determined the spectra of the radical cation of MDMO-PPV and the radical anion of PCNEPV. The former was obtained by recording the PIA spectrum of a blend of MDMO-PPV with a fullerene derivative (PCBM) [Fig. 7(c), dashed line].[36] The absorption of the fullerene (PCBM) anion (at about 1.24 eV) makes an insignificant contribution to the PIA spectrum, because of the much lower absorption coefficient. Hence the PIA spectrum in Fig. 7(c) spectrum shows essentially that of the MDMO-PPV radical cation only.[37] The absorption of the PCNEPV radical anion was determined using a spectroelectrochemical experiment. The differential absorption of PCNEPV at a electrochemical potential of −1.3 V vs Fc/Fc^+ (i.e., in the reduced form) and at 0 V (i.e., in the neutral form) is shown

Fig. 7(c) (solid line). In the reduced (negatively charged) state PCNEPV absorbs strongly at 1.28 and 1.82 eV. The negative signal at 2.82 eV in the differential spectrum [Fig. 7(c)] is a bleaching signal that arises from the depletion of the neutral state of PCNEPV.

Having determined the absorption spectra of MDMO-PPV and PCNEPV in their triplet and charged states, we now turn to the PIA spectrum of their blend. Figure 7(a) shows that in the MDMO-PPV:PCNEPV(1:1 wt) blend, a relatively strong PIA signal is observed at 1.35 eV together with a bleaching band at 2.14 eV, after photoexcitation of both components at 2.70 eV. By comparing the PIA spectra for the blend and the pure materials, the main long-lived induced absorption in the blend can unambiguously be attributed to the MDMO-PPV triplet state. The lifetime of the triplet state in the blend is about 0.1 ms, as inferred from the modulation frequency dependence of the signal intensity. The bleaching at 2.14 eV can also be attributed to MDMO-PPV (see also Fig. 2), supporting the assignment that the long-lived excitations reside on MDMO-PPV and not on PCNEPV. When illuminating the blend with 2.17-eV photons, MDMO-PPV is selectively excited. This results in a PIA signal that is virtually the same as the PIA observed with 2.70-eV excitation where also PCNEPV is excited initially. It is important to note that the intensity of the PIA signal in the blend is higher than in films of pure MDMO-PPV (with identical optical density). Apparently the quantum yield for MDMO-PPV triplet formation is increased in the blend compared to the pure material, despite the fact that the at the same time the photoluminescence MDMO-PPV is strongly quenched and the lifetime of the MDMO-PPV S_1 state is much shorter than 100 ps. The possibility that increased PIA signal results from a longer lifetime in the blend could be ruled out. By measuring the modulation frequency dependence, we verified that the lifetimes associated with the 1.35-eV signals in MDMO-PPV and in the MDMO-PPV:PCNEPV blend are identical (0.1 ms) and much shorter than the modulation cycle ($\sim$2 ms) used to record the spectra in Fig. 7. The increased triplet yield and the simultaneous loss of fluorescence indicate that the long-lived triplet excitations probed by PIA probably do not form directly via intersystem crossing from the MDMO-PPV S_1 state. Instead, we propose that the MDMO-PPV T_1 state evolves from the exciplex state that is formed within 100 ps after excitation (see above).

Thermal annealing of the blend prior to the PIA measurements has only a marginal effect on the PIA spectrum: a slight decrease of the 1.35-eV band and an increase of the signal at $\sim$1.85 eV and the band at 0.50 eV. Comparison of the PIA of the blend and spectra for the charged states of the MDMO-PPV and PCNEPV [Fig. 7(c)] shows that the shoulder around 1.85 eV observed in the annealed MDMO-PPV:PCNEPV blend may be attributed to a low concentration of PCNEPV radical anions. In accordance with charge formation, the additional higher intensity of the PIA band present at 0.50 eV may be attributed to the absorption of the radical cation of the MDMO-PPV.[35] The bleaching, triplet, and radical cation (0.50 eV) PIA signals for the blend all show a very similar sublinear dependence ($\sim I^{0.4-0.5}$) on excitation intensity. The changes in the PIA after thermal annealing are consistent with a higher efficiency for formation of charges (MDMO-PPV$^+$ and PCNEPV$^-$). We note that annealing of the blend results in an increase of the efficiency of photovoltaic energy conversion by a factor of 2.[28] Furthermore, we observe a reduction of the exciplex photoluminescence efficiency by approximately the same factor after annealing.

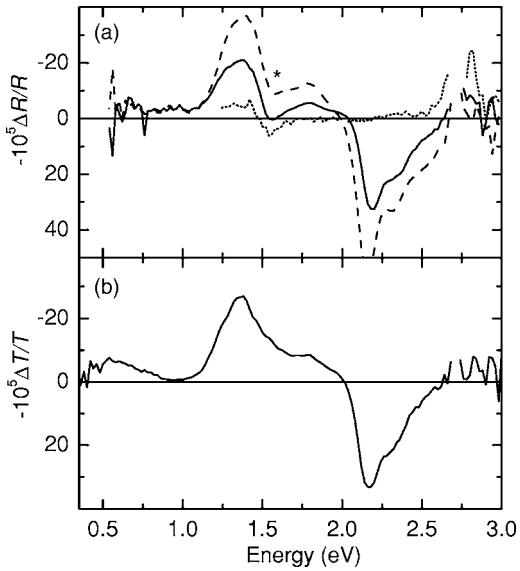

FIG. 8. (a) PIA of an ITO/PEDOT:PSS/MDMO-PPV:PCNEPV/LiF/Al device measured in reflection geometry at different applied voltages: open circuit (solid line), −3 V (dashed line), and +2 V (dotted line). The asterisk indicated the position of the Al thermoreflection feature (see text). (b) PIA of the same film measured adjacent to the LiF/Al electrode but including ITO and PEDOT:PSS. All spectra were recorded at 80 K with excitation at 2.70 eV, using a modulation frequency of 77 Hz.

In Fig. 8 we show results for PIA measurements at 80 K with 77-Hz modulation frequency on MDMO-PPV:PCNEPV blends in photovoltaic devices, i.e., sandwiched between ITO/PEDOT:PSS and LiF/Al electrodes. In the bottom part [Fig. 8(b)] we present the induced absorption including ITO/PEDOT:PSS electrode as measured in the transmission mode. In this measurement the pump and probe beam are focused on an area of the device that is not covered by the LiF/Al back electrode. Comparing the spectrum in Fig. 8(b) with that of the blend on quartz [Fig. 7(a)] we notice a strong similarity. Therefore the main long-lived photoexcitation in the blend is the MDMO-PPV T_1 state, also in the presence of an ITO/PEDOT:PSS electrode.

Because the transmission of the probe light through the photovoltaic device is hampered by the presence of the reflecting LiF/Al electrode, we performed reflection measurements to evaluate the photoinduced absorption. In Fig. 8(a) we show the photoinduced relative differential reflectivity, $\Delta R/R$, on the same device as used for the measurements in Fig. 8(b). One of the problems in measuring photoinduced absorption on devices in reflection geometry is the reduced absorption of light by films on which a metal electrode is evaporated as compared to plain films without electrodes. The reduced absorption is caused by the electromagnetic field being almost zero at the metal electrode.[38] In order to satisfy this condition, the incoming light has to interfere de-

structively with the reflected light wave near the metal surface. This results in very small amplitudes of the electric field of the light ($/\boldsymbol{E}/$) near the electrode that strongly suppresses absorption of light by the polymer near the metal interface. The effect is most noticeable when the wavelength of the light is much larger than the thickness of the film. To correct for this effect, we divide the measured absorption at each wavelength by the $/\boldsymbol{E}/^2$ profile integrated over the film thickness t:[38]

$$\int_0^t \sin^2\left(\frac{2\pi n(\lambda)}{\lambda}x\right)dx. \tag{1}$$

Here $n(\lambda)$ is the wavelength-dependent refractive index of the film.[39] This correction has been carried out on the $\Delta R/R$ spectra shown in Fig. 8(a).

At zero bias we observe a $\Delta R/R$ spectrum that looks rather similar to transmission PIA of the blend [Fig. 7(a)] and the device [Fig. 8(b)]. The main feature at 1.38 eV can be attributed to the T_1 triplet state of MDMO-PPV. This assignment is supported by the bleaching signal at 2.18 eV which can be safely attributed to the depletion of the ground-state absorption of MDMO-PPV. A bleaching of the PCNEPV ground-state absorption is not observed, indicating that the long-lived excitation resides almost exclusively on MDMO-PPV. At the spectral positions corresponding to the strong absorption bands of the MDMO-PPV radical cation (0.50 eV) and the PCNEPV radical anion (1.85 eV) only relatively weak induced absorptions are recorded, showing that the MDMO-PPV$^+$/PCNEPV$^-$ charge-separated state (CSS) is only a minor photoproduct at this time scale.

The $\Delta R/R$ spectrum measured in reflection shows a noticeable dip at 1.56 eV [Fig. 8(a), marked with an asterisk]. We have observed this dip also for films of pure MDMO-PPV with an Al electrode. Careful analysis of the phase and frequency dependence of this signal shows that the dip at 1.56 eV results from an additional ΔR component with a lifetime different from that of the MDMO-PPV T_1 state and with a negative amplitude at 1.56 eV. We assign this component to the thermoreflection effect of Al layers as reported by Rosei.[40] Here it was shown that at certain spectral position, corresponding to an interband transition of Al, the reflectivity of Al changes relatively strongly with temperature. The $\Delta R/R$ spectrum of Al measured at 120 K using a modulated heating power resulting from an ac current through the Al shows a relatively large positive contribution at 1.56 eV, a zero crossing at 1.44 eV, and a negative contribution at 1.30 eV. In our experiments, illumination with the modulated Ar$^+$ laser beam results in formation of various photoexcitations, which eventually decay to the ground state of the system and producing heat. The heat generated in the polymer layer will diffuse to the Al electrode, resulting in a slight temperature change of the Al layer. Eventually, the heat in the polymer and the thin Al layer will diffuse into the thick glass substrate. This one-dimensional heat transport gives rise to thermal excitations that decay in time according to $1/\sqrt{t}$,[41] in agreement with the long-lived nature of the $\Delta R/R$ feature at 1.56 eV in the device.

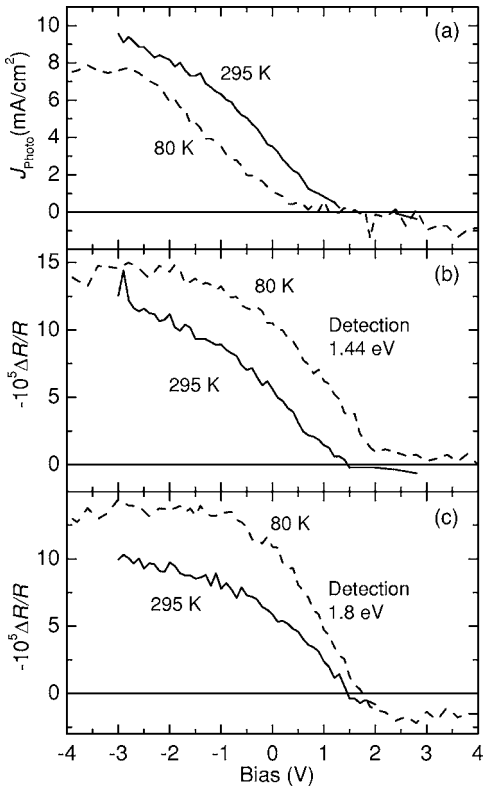

FIG. 9. ITO/PEDOT:PSS/MDMO-PPV:PCNEPV/LiF/Al device under photoexcitation with a modulated (77 Hz) Ar$^+$ laser at 2.70 eV (25 mW, 2-mm-diameter beam). (a) Photocurrent (J_{photo}) as function of applied voltage at 295 K (solid line) and 80 K (dashed line) measured with a white light background illumination of 0.4 W/cm^2. (b) and (c) PIA intensity at 1.44 and 1.80 eV, respectively as function of the applied voltage at 295 K (solid lines) and 80 K (dashed lines).

At +2 V bias, all photoinduced absorption ($\Delta R/R$) bands in the blend are strongly reduced except for the thermoreflectivity feature of the Al layer centered on the 1.44 eV zero crossing [Fig. 8(a)]. Incidentally, this allows us to confirm that the thermoreflectivity feature of the Al electrode makes up only a relatively small component of the induced reflectivity at zero bias. We ascribe the loss of the long-lived PIA signal to quenching of the photogenerated triplet state by injected charge carriers under these conditions. In addition, also precursor states (e.g., the exciplex) of the long-lived triplet state may be quenched by injected carriers. Figure 8(a) also shows the $\Delta R/R$ at negative bias (−3 V). At −3V, the induced reflectivity spectrum shows a similar shape as the spectrum recorded at zero bias, but the amplitude has almost doubled.

To study this remarkable bias voltage dependence of $\Delta R/R$ further, we monitored the photoinduced reflectivity at 1.44 and 1.80 eV as a function of applied bias (Fig. 9). At 1.44 eV, the thermoreflection effect crosses zero, while the MDMO-PPV triplet shows a large absorption cross section at this photon energy. At 1.8 eV the PCNEPV anion shows an intense absorption band. The cells studied here give an open circuit voltage (V_{OC}) of 1.36 V. As can be seen in Fig. 9(b), the induced triplet absorption ($-\Delta R/R$) at 80 K first rises

sharply below V_{OC} with decreasing (more negative) bias and seems to level off for $V<-2$ V. By monitoring the modulation frequency dependence at different bias voltages we verified that the lifetime does not depend on the bias and hence the increase in signal at more negative bias is due to more triplet states. At bias voltages higher than V_{OC}, the induced triplet absorption practically vanishes. Figure 9(c) shows that the PCNEPV radical anion signal at 1.80 eV shows essentially the same behavior. The small positive $\Delta R/R$ signal in Fig. 9(c) under forward bias ($V>V_{OC}$) is due to fluorescence. At room temperature the induced reflectivity at 1.44 and 1.80 eV is considerably smaller than at 80 K because the lifetime of the induced photoexcitations is shorter.

We have also measured the photoinduced current under the same conditions as used in the PIA measurements [Fig. 9(a)]. The mechanically modulated illumination (2.70 eV, 0.8 W/cm^2, 77 Hz) allows for standard lock-in detection of the current. Here the amplitude and phase of the current as a function of bias and modulation frequency are measured. The photocurrent was found to be in phase with the laser light at the modulation frequency used for all bias voltages used, except for voltages $>V_{OC}$ under forward bias at 80 K where a small phase lag on the order of 10° is observed. The absence of an appreciable phase lag shows that the transit time of the majority of photogenerated charge carriers must be considerably shorter than the period of the modulation cycles ($\sim$10 ms) even at 80 K.

In Fig. 9(a) we show the amplitude of the photocurrent as a function of bias voltage. For voltages above V_{OC}, the amplitude of the photocurrent is much smaller than for voltages below V_{OC}. When applying voltages above V_{OC} to the device, a significant number of charge carriers are injected through the contacts. From electromodulation spectroscopy on polymer light-emitting diodes it was recently inferred that under forward bias, the internal electric field in the device is effectively screened by accumulation of trapped electrons at the PEDOT:PSS electrode.[42] A similar effect in our diodes could explain the loss of photocurrent for $V>V_{OC}$. Due to the low electric field inside the device, excitations would not dissociate into free carriers. In addition, the reduction of the photocurrent for $V>V_{OC}$ may result from annihilation of either the precursor states of the carriers or the carriers themselves by charge carriers injected through the electrodes. The observation of electroluminescence for $V>V_{OC}$ indicates that quenching of the exciplex state by injected carriers plays only a minor role. For voltages below V_{OC}, the number of injected carriers is of course negligible and quenching of excitations by injected carriers may be neglected.

With increasing reverse bias, the photocurrent slowly increases and reaches its maximum value only at very low bias voltages. This shows that the efficiency of the collection of photoinduced charge carriers strongly depends on the bias. Upon reducing the temperature the short-circuit current (J_{SC}) drops by a factor of 3.2. This shows that the efficiency is also strongly temperature dependent. At low temperature J_{SC} increases slowly with increasing negative bias and saturates for voltages below -2.5 V. At -2.5 V, the ratio between the photocurrent measured at 295 and 80 K is much smaller than the ratio at zero bias. This indicates that the relatively high electric field can compensate the reduction in efficiency resulting from the lower thermal energy at 80 K.

IV. DISCUSSION

A. Energy of the exciplex

From extensive research on mixtures of small aromatic molecules with electron donating and electron accepting properties it is well known that photoexcitation of one of the two components may cause the formation of an exciplex between the (photoexcited) donor and acceptor in which there is partial charge transfer. Exciplex formation is to be expected when the difference of the electron affinity of the electron accepting molecule (EA_A) and the ionization potential of the electron donating molecule (IP_D) is comparable to the energy of the lowest excited singlet state of either the donor or acceptor. In some cases luminescence is observed from the exciplex, which allows for a direct determination of its energy. A linear correlation between the photon energy at the maximum of the exciplex emission band (when hexane is used as solvent) and the quantity EA_A-IP_D has been observed:[21]

$$h\nu_{ems}^{\max}(\text{hexane}) = [IP_D - EA_A] - \Delta. \tag{2}$$

The difference EA_A-IP_D is usually determined from cyclic voltammetry (CV) measurements and corresponds to the energy needed to create an electron-hole pair with infinite separation in the solvent used for CV. The exciplex may in first approximation be regarded as an electron-hole pair at close distance. The energy of the exciplex is expected to be equal to EA_A-IP_D plus an additional (negative) term describing the Coulombic binding energy of the electron and hole in the exciplex which may be estimated at a few tenths of eV. For couples of relatively strong donors and acceptors, the experimental value for Δ, which may represent the Coulombic potential energy, is, however, quite small: 0.1 ± 0.08 eV.[21] The small value observed for Δ is usually interpreted in terms of a partial cancellation of the Coulombic term by the high solvation energy of the charges in the polar solvents used for CV.

For the PCNEPV and MDMO-PPV polymers under study here, EA_A-IP_D amounts to 1.81 eV,[28] which is close in energy to the MDMO-PPV S_1 state (2.1 eV). The excimer has its maximum emission intensity at 1.85 eV and therefore the empirical correlation (2) seems to hold also for this set of polymers.

Another empirical correlation that may be made concerns V_{OC} and EA_A-IP_D. For the well-known MDMO-PPV/PCBM solar cells a V_{OC} of 0.9 V (Ref. 12) is observed using Al and PEDOT:PSS as electrodes. EA_A-IP_D amounts to 1.3 eV and the observed difference between EA_A-IP_D and V_{OC} is 0.4 eV (which has been rationalized in terms of a loss of two times 0.2 eV caused by band bending effects at the electrodes[43]). This correlation between EA_A-IP_D and V_{OC} holds for a number of polymer donor-acceptor combinations.[44] Also the open circuit voltage of 1.36 V for the MDMO-PPV:PCNEPV bulk heterojunctions matches well with $[EA_A-IP_D]-0.4$ V$=1.4$ V.

Charge carriers in a molecular solid can be stabilized by electronic polarization of the molecules surrounding the charge carrier. The energies involved are considerable (e.g., 0.8 eV predicted for electrons in an α-sexithiophene crystal[45]). To estimate the energy of the charge separated state for a molecular material from CV measurements requires evaluation of the difference in polarization and solvation energies of the charge carriers in the material and the solvent used for CV. In practice this is very difficult.

The polarization stabilization of an exciplex is expected to be much less than the sum of the polarization stabilizations of the infinitely separated electron-hole pair. Therefore in molecular solids, the energy of an electron-hole pair with a distance between carriers sufficiently large to profit from the polarization energy of the material and small enough to still have some stabilization due to the Coulomb interaction, may in principle be lower than that of the exciplex state.

For the polymers under study here, the experimental observation of electrogenerated exciplex luminescence at low temperature (T=80 K) shows that the energy of electron-hole pairs must either be higher or comparable in energy (±0.04 eV) to the exciplex state, as electron-hole pairs spontaneously combine to form the exciplex state. Assuming the electron-hole pair states to be slightly higher in energy than the exciplex state, the rise of the quantum yield for exciplex luminescence upon lowering the temperature and the lengthening of its luminescence lifetime follow naturally. This assumption together with the relatively short lifetime of the exciplex in the absence of any applied field imply that efficient decay channels exist to states other than charge separated states. The existence of such channels would not be consistent with a very high photovoltaic efficiency. However, experimental values for the IPCE of unannealed films as studied with luminescence spectroscopy amount to 8–10 % only and therefore seem compatible with charge pair states being slightly higher in energy than the exciplex state.

To illustrate the photophysical processes that may occur in the blend of polymers, we show an energy diagram in Fig. 10 that illustrates the energetic position of various states. The strong quenching of the fluorescence of MDMO-PPV shows that its S_1 state decays rapidly into an exciplex or into a charge-separated state (CSS). In the diagram we assume that the MDMO-PPV$^+$/PCNEPV$^-$ charge-separated state (CSS) with charges at a large distance has a higher energy than the exciplex state and that work has to be performed to separate the charges against the Coulombic attraction force. The energy of the MDMO-PPV T_1 state is at ~1.3 eV.[46]

B. Dissociation of the exciplex in an electric field

The exciplex may dissociate into free charge carriers under the influence of an electric field. Experimental evidence for this field-induced exciplex dissociation comes from two experiments: (i) the photocurrent measurements and (ii) the emission lifetime and intensity measurements at variable bias. The probability for exciplex dissociation is also expected to depend on the available thermal energy. Indeed, we observe that at a given reverse voltage, the photocurrent at low temperature is smaller than at room temperature. The

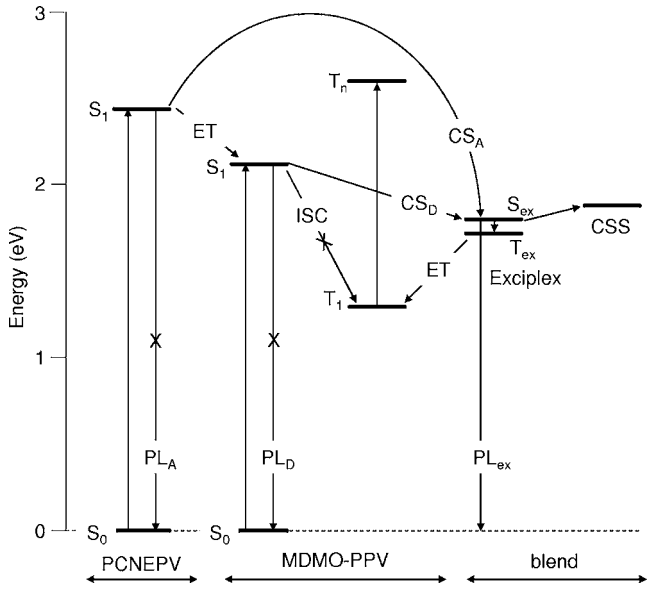

FIG. 10. State energy diagram of the various singlet (S), triplet (T), exciplex (ex), and charge-separated (CSS) states in the donor (D)–acceptor (A) blend of MDMO-PPV and PCNEPV; and transitions (ET=energy transfer; CS=charge separation; PL=photoluminescence; ISC=intersystem crossing) between these states. Crosses indicate processes that do occur in the pure materials, but that are quenched in the blend.

fact that the photocurrent at very high reverse voltage reaches similar values for both high and low temperature indicates that the smaller thermal energy available for exciplex dissociation at low temperatures can be compensated by a higher applied field.

Exciplex states can have either a singlet or triplet spin signature (S_{ex} and T_{ex} in Fig. 10). The triplet exciplex state is expected to be lower in energy than the singlet due to its exchange correlation. When the overlap between the orbitals occupied by the electron and the hole is large, the energy separating the singlet and triplet exciplex levels (ΔE_{ST}) is considerable. Here we assume that for the exciplex at the interface between the MDMO-PPV and PCNEPV polymer phases, a considerable ΔE_{ST} exists ($\gg k_B T$). For the charge separated state (CSS; see Fig. 10) the overlap between the orbitals occupied by the electron and hole will be very small, especially when the carriers are far apart. This results in a vanishingly small energy splitting between singlet and triplet levels when the charge carriers are far apart. When the CSS state is formed out of another state with particular spin quantum numbers, the mutual coherence between the separated spins originating from the parent state is lost rapidly due to thermal fluctuations. Here the relevant time scale is the spin dephasing time ($\sim\mu$s). Thus a relatively long-lived CSS state with its electron and hole far apart can best be described as a diradical with the two spins behaving independently.

Due to the forbidden nature of transitions between singlet states and triplet states, the most likely state to be formed from the MDMO-PPV S_1 or PCNEPV S_1 states is the singlet exciplex state (S_{ex}, see Fig. 10). Similarly, decay of the singlet exciplex to the MDMO-PPV T_1 or to the PCNEPV T_1 is also spin forbidden, leading to only a small yield for these

triplet states. Interestingly, picosecond photoinduced absorption spectroscopy confirms that triplet formation occurs only with low yield on short time scale. From the near-steady-state PIA measurements we know that the T_1 of the polymers absorbs relatively strongly at 1.27 eV whereas it absorption at 0.56 eV is vanishingly small. The cross sections for photon absorption at the maxima of the absorption bands are approximately equally large for the triplet and the charged states of the conjugated polymers. This follows from referencing differential absorption spectra of the triplet and the charged states to the magnitude of the bleaching band. The fast photoinduced absorption traces at 1.27 and 0.56 eV are, however, almost identical showing that in the 0–700-ps time window no significant formation of MDMO-PPV T_1 states occurs. If this would have occurred, the absorption trace at 1.27 eV should decay more slowly than the trace recorded at 0.56 eV probe energy.

C. Electric-field enhanced triplet formation

To explain the rise of the triplet absorption spectrum in the devices under influence of the electric field we reason as follows. The electric field assists in separating the hole and electron comprising the exciplex. This can result in formation of free carriers, as is evidenced by the rise in the photocurrent. A significant fraction of the carriers may, however, still recombine because the carriers do not have enough energy to escape from the Coulombic attraction. During this process, the charge-carrier pair will have existed for a while as a weakly bound electron-hole pair with the two spins far apart. As discussed above the spin state of such a widely separated electron-hole pair can be viewed as a diradical provided that the lifetime of the separated state is long in comparison with the spin dephasing time. The separated electron-hole pair may then collapse again to form a triplet state; the transition from the diradical CSS state to a triplet state is not spin forbidden and should occur with a probability of 0.75 in first approximation. This indirect route for triplet formation may be more efficient than the direct route for intersystem crossing of the exciplex singlet state to the triplet state ($S_1 \rightarrow T_1$) resulting in a field-dependent efficiency for triplet formation.[47]

At high electric fields, one may expect that the photogenerated charge carriers will be swept out of the device before they can recombine to the triplet state and hence one may predict a reduction of the yield of triplets at high electric fields.[48] The experimental data do not show such a reduction in the range of electric fields studied. We remark that even for some of the most efficient polymer solar cells known, namely the MDMO-PPV-fullerene bulk hetero junction cells, only 60% of the charge carriers are swept out of the device under short-circuit conditions. Even for these optimized cells, electric fields with strength $E > 8 \times 10^5$ V/cm are needed for quantitative collection of charge carriers.[49] Sweeping out the charge carriers before they can recombine implies a rate for escape of a charge carrier from the geminate pair equal to the attempt frequency for escape. The absence of a reduction of the triplet yield at high fields may therefore be rationalized in terms of relatively steep potential well for the geminate pair with a high attempt frequency for escape, high probability for formation of the triplet for each attempted escape and low probability for escape per attempt.

V. CONCLUSIONS

The open-circuit voltage of photovoltaic devices with a polymer-polymer bulk heterojunction may be increased by choosing a combination of materials in which the charge-separated state has a high energy. The simple design rule to increase the open-circuit voltage is to increase the difference $EA_A - IP_D$. The present study confirms this design rule through the observation of a relatively high open-circuit voltage (1.36 V) for photovoltaic devices with the MDMO-PPV:PCNEPV blend as active layer.

A charge-separated state that is high in energy and therefore closer to the energy of the lowest excited singlet states of the polymers allows for radiative decay of the exciplex resulting from admixture of the lowest excited singlet states to the charge-separated state. For the MDMO-PPV:PCNEPV blend we have indeed found compelling evidence for the occurrence of such an exciplex state. Temperature-dependent measurements show that an electric field assists in the dissociation of the exciplex into "free" charge carriers. A drawback of a combination of donor and acceptor polymers featuring a high-energy intermolecular charge-separated state is that this state is higher than the lowest triplet state of the polymer, which allows for recombination of electrons and holes to form a triplet exciton. This process was identified in MDMO-PPV:PCNEPV blends where the yield of MDMO-PPV triplets was higher than in pure MDMO-PPV and increased with the applied electric field across the layer. The observation of this field-dependent triplet formation demonstrates that spin selection rules, in combination with the strong Coulombic attraction between holes and electrons at the active interface, can play an important role in the recombination kinetics of photoinduced charges in polymer photovoltaics. From the perspective of photovoltaic energy conversion, this could be a disadvantage because triplet formation may present a significant loss channel.

ACKNOWLEDGMENTS

We thank Dr. Eric Levillain (DR2 CNRS), Groupe Systemes Conjugues Lineaires, CIMMA, UMR 6200, in Angers University (France) for spectroelectrochemistry and Dr. Martijn Wienk, Dr. Sjoerd Veenstra, and Dr. Jan Kroon for valuable discussions. The work of TO and MMK forms part of the research program of the Dutch Polymer Institute (DPI), Project Nos. DPI 324 and 325, respectively. The materials used for this research were synthesized by J. Sweelssen (TNO/DPI). The research of S.C.J.M. has been made possible by the Royal Dutch Academy of Arts and Sciences.

*Electronic address: s.c.j.meskers@tue.nl

[1] R. Kersting, U. Lemmer, M. Deussen, H. J. Bakker, R. F. Mahrt, H. Kurz, V. I. Arkhipov, H. Bässler, and E. O. Göbel, Phys. Rev. Lett. **73**, 1440 (1994).

[2] J. J. M. Halls, C. A. Walsh, N. C. Greenham, E. A. Marseglia, R. H. Friend, S. C. Moratti, and A. B. Holmes, Nature (London) **376**, 498 (1995).

[3] G. Yu, J. C. Hummelen, F. Wudl, and A. J. Heeger, Science **270**, 1789 (1995).

[4] S. E. Shaheen, C. J. Brabec, N. S. Sariciftci, F. Padinger, T. Fromherz, and J. C. Hummelen, Appl. Phys. Lett. **78**, 841 (2001).

[5] F. Padinger, R. S. Rittberger, and N. S. Sariciftci, Adv. Funct. Mater. **13**, 85 (2003).

[6] P. Schilinsky, C. Waldauf, and C. J. Brabec, Appl. Phys. Lett. **81**, 3885 (2002).

[7] M. M. Wienk, J. M. Kroon, W. J. H. Verhees, J. Knol, J. C. Hummelen, P. A. van Hal, and R. A. J. Janssen, Angew. Chem., Int. Ed. **42**, 3371 (2003).

[8] A. C. Arias, J. D. MacKenzie, R. Stevenson, J. J. M. Halls, M. Inbasekaran, E. P. Woo, D. Richards, and R. H. Friend, Macromolecules **34**, 6005 (2001).

[9] J. J. M. Halls, A. C. Arias, J. D. MacKenzie, W. Wu, M. Inbasekaran, E. P. Woo, and R. H. Friend, Adv. Mater. (Weinheim, Ger.) **12**, 498 (2000).

[10] H. J. Snaith, A. C. Arias, A. C. Morteani, C. Silva, and R. H. Friend, Nano Lett. **2**, 1353 (2002).

[11] T. Martens, T. Munters, L. Goris, K. Schoutenden, M. d'Olieslaeger, L. Lutsen, D. Vanderzande, W. Geens, J. Poortmans, L. de Schepper, and J. V. Manca, Appl. Phys. A: Mater. Sci. Process. **79**, 27 (2004).

[12] J. K. J. van Duren, X. Yang, J. Loos, C. W. T. Bulle-Lieuwma, A. B. Sieval, J. C. Hummelen, and R. A. J. Janssen, Adv. Funct. Mater. **14**, 425 (2004).

[13] S. Barth, D. Hertel, Y. H. Tak, H. Bässler, and H. H. Hörhold, Chem. Phys. Lett. **274**, 165 (1997).

[14] J. Nelson, Phys. Rev. B **67**, 155209 (2003).

[15] T. Offermans, S. C. J. Meskers, and R. A. J. Janssen, J. Chem. Phys. **119**, 10924 (2003).

[16] V. I. Arkhipov, P. Heremans, and H. Bässler, Appl. Phys. Lett. **82**, 4605 (2003).

[17] T. Offermans, S. C. J. Meskers, and R. A. J. Janssen, Chem. Phys. **308**, 125 (2005).

[18] P. Peumans and S. R. Forrest, Chem. Phys. Lett. **398**, 27 (2004).

[19] V. D. Mihailetchi, L. J. A. Koster, J. C. Hummelen, and P. W. M. Blom, Phys. Rev. Lett. **93**, 216601 (2004).

[20] A. Weller, in *The Exciplex*, edited by M. Gordon and W. Ware (Academic, New York, 1975), pp. 23–28.

[21] H. Beens and A. Weller, in *Organic Molecular Photophysics*, edited by J. B. Birks (Wiley, London, 1975), Vol. 2, Chap. 4, pp. 159–215.

[22] A. C. Morteani, A. S. Dhoot, J. S. Kim, C. Silva, N. C. Greenham, C. Murphy, E. Moons, S. Cina, and R. H. Friend, Adv. Mater. (Weinheim, Ger.) **15**, 1708 (2003).

[23] A. C. Morteani, P. Sreearunothai, L. M. Herz, R. H. Friend, and C. Silva, Phys. Rev. Lett. **92**, 247402 (2004).

[24] S. Wang and G. C. Bazan, Chem. Phys. Lett. **333**, 437 (2001).

[25] H. Tillmann and H. H. Hörhold, Synth. Met. **101**, 138 (1999).

[26] M. M. Koetse, J. Sweelssen, T. Franse, S. C. Veenstra, J. M. Kroon, X. Yang, A. Alexeev, J. Loos, U. S. Schubert, and H. F. M. Schoo, Proc. SPIE **5215**, 119 (2004).

[27] A. J. Breeze, Z. Schlesinger, S. A. Carter, H. Tillman, and H. H. Hörhold, Sol. Energy Mater. Sol. Cells **83**, 2004 (263).

[28] S. C. Veenstra, W. J. H. Verhees, J. M. Kroon, M. M. Koetse, J. Sweelssen, J. A. J. M. Bastiaansen, H. F. M. Schoo, X. Yang, A. Alexeev, J. Loos, U. S. Schubert, and M. M. Wienk, J. Mater. Chem. **16**, 2503 (2004).

[29] L. Lutsen, P. Adriaensens, H. Becker, A. J. van Breemen, D. Vanderzande, and J. Gelan, Macromolecules **32**, 6517 (1999).

[30] C. Im, H. Bässler, H. Rost, and H. H. Hörhold, J. Chem. Phys. **113**, 3802 (2000).

[31] N. C. Greenham, J. Shinar, J. Partee, P. A. Lane, O. Amir, F. Lu, and R. H. Friend, Phys. Rev. B **53**, 13528 (1996).

[32] I. D. W. Samuel, G. Rumbles, and C. J. Collison, Phys. Rev. B **52**, R11573 (1995).

[33] I. H. Campbell, T. W. Hagler, D. L. Smith and J. P. Ferraris, Phys. Rev. Lett. **76**, 1900 (1996)

[34] M. C. Scharber, N. A. Schultz, N. S. Sariciftci, and C. J. Brabec, Phys. Rev. B **67**, 085202 (2003).

[35] G. Zerza, R. Röthler, N. S. Sariciftci, R. Gomez, J. L. Segura, and N. Martin, J. Phys. Chem. B **105**, 4099 (2001).

[36] M. C. Scharber, C. Winder, H. Neugebauer, and N. S. Sariciftci, Synth. Met. **141**, 109 (2004).

[37] D. M. Guldi and M. Prato, Acc. Chem. Res. **33**, 695 (2000).

[38] H. Hansel, H. Zettl, G. Krausch, R. Kisselev, M. Thelakkat, and H. W. Schmidt, Adv. Mater. (Weinheim, Ger.) **15**, 2056 (2003).

[39] C. M. Ramsdale and N. C. Greenham, Adv. Mater. (Weinheim, Ger.) **14**, 212 (2002).

[40] R. Rosei and D. W. Lynch, Phys. Rev. B **5**, 3883 (1972).

[41] S. C. J. Meskers, J. K. J. van Duren, and R. A. J. Janssen, J. Appl. Phys. **92**, 7041 (2002).

[42] P. A. Lane, J. C. deMello, R. B. Fletcher, and M. Bernius, Appl. Phys. Lett. **83**, 3611 (2003).

[43] V. D. Mihailetchi, P. W. M. Blom, J. C. Hummelen, and M. T. Rispens, J. Appl. Phys. **94**, 6849 (2003).

[44] C. J. Brabec, A. Cravino, D. Meissner, N. S. Sariciftci, M. T. Rispens, L. Sanchez, J. C. Hummelen, and T. Fromherz, Thin Solid Films **403-404**, 368 (2002).

[45] M. Andrzejak and P. Petelenz, Synth. Met. **109**, 97 (2000).

[46] A. P. Monkman, H. D. Burrows, L. J. Hartwell, L. E. Horsburgh, I. Hamblett, and S. Navaratnam, Phys. Rev. Lett. **86**, 1358 (2001).

[47] Using calculated values for the absorption cross section of the triplet-triplet absorption band for PPV-type polymers (10^{-15} cm^2, Ref. 48) one may estimate the quantum efficiency for formation of the triplet state in a film of the MDMO-PPV/PCNEPV blend (Fig. 7). Using the experimentally determined value for the lifetime of the triplet state (0.1 ms) and neglecting bimolecular triplet-triplet deactivation mechanisms, one estimates the overall quantum yield for formation of the triplet at a few percent. This indicates that formation of triplet states can be a significant loss mechanism during photovoltaic operation of the bulk heterojunction polymer blend.

[48] T. A. Ford, I. Avilov, D. Beljonne, and N. C. Greenham, Phys. Rev. B **71**, 125212 (2005).

[49] V. D. Mihailetchi, L. J. A. Koster, J. C. Hummelen, and P. W. M. Blom, Phys. Rev. Lett. **93**, 216601 (2004).